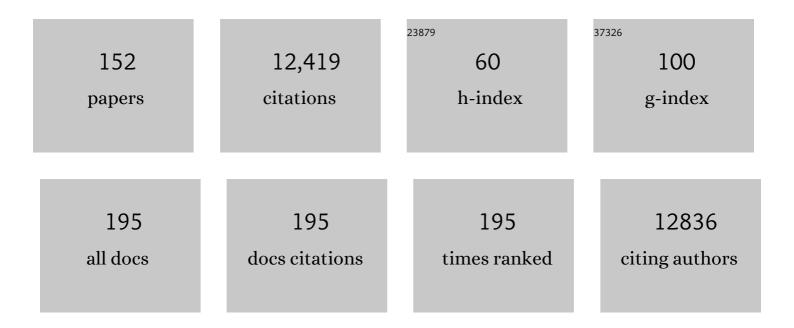
Grant Jensen

List of Publications by Year in descending order

Source: https://exaly.com/author-pdf/7926250/publications.pdf Version: 2024-02-01



#	Article	IF	CITATIONS
1	UVC inactivation of pathogenic samples suitable for cryo-EM analysis. Communications Biology, 2022, 5, 29.	2.0	7
2	Novel transient cytoplasmic rings stabilize assembling bacterial flagellar motors. EMBO Journal, 2022, 41, e109523.	3.5	10
3	Cryo-electron tomography of the onion cell wall shows bimodally oriented cellulose fibers and reticulated homogalacturonan networks. Current Biology, 2022, 32, 2375-2389.e6.	1.8	29
4	Montage electron tomography of vitrified specimens. Journal of Structural Biology, 2022, 214, 107860.	1.3	20
5	Structure of the Bacterial Cellulose Ribbon and Its Assembly-Guiding Cytoskeleton by Electron Cryotomography. Journal of Bacteriology, 2021, 203, .	1.0	31
6	Simulations of Proposed Mechanisms of FtsZ-Driven Cell Constriction. Journal of Bacteriology, 2021, 203, .	1.0	5
7	A cryo–electron tomography workflow reveals protrusion-mediated shedding on injured plasma membrane. Science Advances, 2021, 7, .	4.7	13
8	Measuring gas vesicle dimensions by electron microscopy. Protein Science, 2021, 30, 1081-1086.	3.1	20
9	Challenges in solving structures from radiation-damaged tomograms of protein nanocrystals assessed by simulation. Acta Crystallographica Section D: Structural Biology, 2021, 77, 572-586.	1.1	0
10	Moltemplate: A Tool for Coarse-Grained Modeling of Complex Biological Matter and Soft Condensed Matter Physics. Journal of Molecular Biology, 2021, 433, 166841.	2.0	189
11	Loss of the Bacterial Flagellar Motor Switch Complex upon Cell Lysis. MBio, 2021, 12, e0029821.	1.8	6
12	Programmed Flagellar Ejection in Caulobacter crescentus Leaves PL-subcomplexes. Journal of Molecular Biology, 2021, 433, 167004.	2.0	7
13	Rapid tilt-series method for cryo-electron tomography: Characterizing stage behavior during FISE acquisition. Journal of Structural Biology, 2021, 213, 107716.	1.3	14
14	Generation of ordered protein assemblies using rigid three-body fusion. Proceedings of the National Academy of Sciences of the United States of America, 2021, 118, .	3.3	25
15	In situ imaging of bacterial outer membrane projections and associated protein complexes using electron cryo-tomography. ELife, 2021, 10, .	2.8	16
16	<i>The Atlas of Bacterial & Archaeal Cell Structure</i> : an Interactive Open-Access Microbiology Textbook. Journal of Microbiology and Biology Education, 2021, 22, .	0.5	6
17	The stress-sensing domain of activated IRE1α forms helical filaments in narrow ER membrane tubes. Science, 2021, 374, 52-57.	6.0	24
18	In Situ Imaging and Structure Determination of Biomolecular Complexes Using Electron Cryo-Tomography. Methods in Molecular Biology, 2021, 2215, 83-111.	0.4	9

#	Article	IF	CITATIONS
19	A bacterial membrane sculpting protein with BAR domain-like activity. ELife, 2021, 10, .	2.8	6
20	Effects of antimicrobial photodynamic therapy on antibiotic-resistant Escherichia coli. Photodiagnosis and Photodynamic Therapy, 2020, 32, 102029.	1.3	20
21	Correlated cryogenic fluorescence microscopy and electron cryo-tomography shows that exogenous TRIM51 [±] can form hexagonal lattices or autophagy aggregates in vivo. Proceedings of the National Academy of Sciences of the United States of America, 2020, 117, 29702-29711.	3.3	20
22	PilY1 and minor pilins form a complex priming the type IVa pilus in Myxococcus xanthus. Nature Communications, 2020, 11, 5054.	5.8	67
23	CryoEM structure of the type IVa pilus secretin required for natural competence in Vibrio cholerae. Nature Communications, 2020, 11, 5080.	5.8	21
24	Visualizing insulin vesicle neighborhoods in β cells by cryo–electron tomography. Science Advances, 2020, 6, .	4.7	27
25	Repurposing a chemosensory macromolecular machine. Nature Communications, 2020, 11, 2041.	5.8	38
26	Bacterial flagellar motor PL-ring disassembly subcomplexes are widespread and ancient. Proceedings of the United States of America, 2020, 117, 8941-8947.	3.3	23
27	Ribosome-associated vesicles: A dynamic subcompartment of the endoplasmic reticulum in secretory cells. Science Advances, 2020, 6, eaay9572.	4.7	42
28	Qualitative Analyses of Polishing and Precoating FIB Milled Crystals for MicroED. Structure, 2019, 27, 1594-1600.e2.	1.6	33
29	In Situ Imaging and Structure Determination of Bacterial Toxin Delivery Systems Using Electron Cryotomography. Methods in Molecular Biology, 2019, 1921, 249-265.	0.4	7
30	Collection of Continuous Rotation MicroED Data from Ion Beam-Milled Crystals of Any Size. Structure, 2019, 27, 545-548.e2.	1.6	58
31	<i>In situ</i> imaging of the bacterial flagellar motor disassembly and assembly processes. EMBO Journal, 2019, 38, e100957.	3.5	43
32	Fusion of DARPin to Aldolase Enables Visualization of Small Protein by Cryo-EM. Structure, 2019, 27, 1148-1155.e3.	1.6	32
33	ETDB-Caltech: A blockchain-based distributed public database for electron tomography. PLoS ONE, 2019, 14, e0215531.	1.1	37
34	Simulations suggest a constrictive force is required for Gram-negative bacterial cell division. Nature Communications, 2019, 10, 1259.	5.8	12
35	Molecular architecture, polar targeting and biogenesis of the Legionella Dot/Icm T4SS. Nature Microbiology, 2019, 4, 1173-1182.	5.9	80
36	FGF21 trafficking in intact human cells revealed by cryo-electron tomography with gold nanoparticles. ELife, 2019, 8, .	2.8	25

#	Article	IF	CITATIONS
37	Electron Cryotomography of Bacterial Secretion Systems. Microbiology Spectrum, 2019, 7, .	1.2	13
38	De Novo Structural Pattern Mining in Cellular Electron Cryotomograms. Structure, 2019, 27, 679-691.e14.	1.6	40
39	Distinct Chemotaxis Protein Paralogs Assemble into Chemoreceptor Signaling Arrays To Coordinate Signaling Output. MBio, 2019, 10, .	1.8	10
40	Bacterial Swarming Reduces Proteus mirabilis and Vibrio parahaemolyticus Cell Stiffness and Increases β-Lactam Susceptibility. MBio, 2019, 10, .	1.8	17
41	In vivo structure of the Legionella type II secretion system by electron cryotomography. Nature Microbiology, 2019, 4, 2101-2108.	5.9	43
42	Rapid tilt-series acquisition for electron cryotomography. Journal of Structural Biology, 2019, 205, 163-169.	1.3	85
43	The presence and absence of periplasmic rings in bacterial flagellar motors correlates with stator type. ELife, 2019, 8, .	2.8	36
44	Electron cryotomography of <i>Mycoplasma pneumoniae</i> mutants correlates terminal organelle architectural features and function. Molecular Microbiology, 2018, 108, 306-318.	1.2	15
45	Acoustically modulated magnetic resonance imaging of gas-filled protein nanostructures. Nature Materials, 2018, 17, 456-463.	13.3	88
46	Recombinantly expressed gas vesicles as nanoscale contrast agents for ultrasound and hyperpolarized MRI. AICHE Journal, 2018, 64, 2927-2933.	1.8	39
47	InÂVivo Structures of the Helicobacter pylori cag Type IV Secretion System. Cell Reports, 2018, 23, 673-681.	2.9	80
48	Structure of the fission yeast actomyosin ring during constriction. Proceedings of the National Academy of Sciences of the United States of America, 2018, 115, E1455-E1464.	3.3	38
49	Ultrastructure of <i>Shewanella oneidensis</i> MR-1 nanowires revealed by electron cryotomography. Proceedings of the National Academy of Sciences of the United States of America, 2018, 115, E3246-E3255.	3.3	151
50	Distinguishing signal from autofluorescence in cryogenic correlated light and electron microscopy of mammalian cells. Journal of Structural Biology, 2018, 201, 15-25.	1.3	27
51	Programmed Secretion Arrest and Receptor-Triggered Toxin Export during Antibacterial Contact-Dependent Growth Inhibition. Cell, 2018, 175, 921-933.e14.	13.5	71
52	Selective Permeability of Carboxysome Shell Pores to Anionic Molecules. Journal of Physical Chemistry B, 2018, 122, 9110-9118.	1.2	54
53	Coarse-grained simulations of actomyosin rings point to a nodeless model involving both unipolar and bipolar myosins. Molecular Biology of the Cell, 2018, 29, 1318-1331.	0.9	19
54	Nutrient transport suggests an evolutionary basis for charged archaeal surface layer proteins. ISME Journal, 2018, 12, 2389-2402.	4.4	51

#	Article	IF	CITATIONS
55	Architecture of the Vibrio cholerae toxin-coregulated pilus machine revealed by electron cryotomography. Nature Microbiology, 2017, 2, 16269.	5.9	67
56	Polyphosphate granule biogenesis is temporally and functionally tied to cell cycle exit during starvation in <i>Pseudomonas aeruginosa</i> . Proceedings of the National Academy of Sciences of the United States of America, 2017, 114, E2440-E2449.	3.3	93
57	Progress and Potential of Electron Cryotomography as Illustrated by Its Application to Bacterial Chemoreceptor Arrays. Annual Review of Biophysics, 2017, 46, 1-21.	4.5	23
58	Cellular Electron Cryotomography: Toward Structural Biology In Situ. Annual Review of Biochemistry, 2017, 86, 873-896.	5.0	138
59	Short FtsZ filaments can drive asymmetric cell envelope constriction at the onset of bacterial cytokinesis. EMBO Journal, 2017, 36, 1577-1589.	3.5	55
60	The Structure, Function and Roles of the Archaeal ESCRT Apparatus. Sub-Cellular Biochemistry, 2017, 84, 357-377.	1.0	23
61	<i>In vivo</i> structures of an intact type <scp>VI</scp> secretion system revealed by electron cryotomography. EMBO Reports, 2017, 18, 1090-1099.	2.0	64
62	Uncharacterized Bacterial Structures Revealed by Electron Cryotomography. Journal of Bacteriology, 2017, 199, .	1.0	49
63	<i>In situ</i> structure of the <i>Legionella</i> Dot/Icm type <scp>IV</scp> secretion system by electron cryotomography. EMBO Reports, 2017, 18, 726-732.	2.0	101
64	Giant viruses with an expanded complement of translation system components. Science, 2017, 356, 82-85.	6.0	234
65	The Variable Internal Structure of the Mycoplasma penetrans Attachment Organelle Revealed by Biochemical and Microscopic Analyses: Implications for Attachment Organelle Mechanism and Evolution. Journal of Bacteriology, 2017, 199, .	1.0	10
66	Dynamics of the peptidoglycan biosynthetic machinery in the stalked budding bacterium <i>Hyphomonas neptunium</i> . Molecular Microbiology, 2017, 103, 875-895.	1.2	35
67	LytM factors affect the recruitment of autolysins to the cell division site in <i>Caulobacter crescentus</i> . Molecular Microbiology, 2017, 106, 419-438.	1.2	26
68	Preparation of biogenic gas vesicle nanostructures for use as contrast agents for ultrasound and MRI. Nature Protocols, 2017, 12, 2050-2080.	5.5	116
69	Morphology of the archaellar motor and associated cytoplasmic cone in <i>Thermococcus kodakaraensis</i> . EMBO Reports, 2017, 18, 1660-1670.	2.0	34
70	Photonâ€Induced Nearâ€Field Electron Microscopy of Eukaryotic Cells. Angewandte Chemie, 2017, 129, 11656-11659.	1.6	0
71	The development of cryo-EM and how it has advanced microbiology. Nature Microbiology, 2017, 2, 1577-1579.	5.9	8
72	Assigning chemoreceptors to chemosensory pathways in <i>Pseudomonas aeruginosa</i> . Proceedings of the United States of America, 2017, 114, 12809-12814.	3.3	72

#	Article	IF	CITATIONS
73	Polar delivery of <i>Legionella</i> type IV secretion system substrates is essential for virulence. Proceedings of the National Academy of Sciences of the United States of America, 2017, 114, 8077-8082.	3.3	55
74	Starvation and recovery in the deepâ€sea methanotroph <scp><i>M</i></scp> <i>ethyloprofundus sedimenti</i> . Molecular Microbiology, 2017, 103, 242-252.	1.2	40
75	Electron Cryotomography of Vitreous Cryosections and Cryo-Focused Ion Beam Milled Lamellae Microscopy and Microanalysis, 2017, 23, 2314-2315.	0.2	0
76	FtsEX-mediated regulation of the final stages of cell division reveals morphogenetic plasticity in Caulobacter crescentus. PLoS Genetics, 2017, 13, e1006999.	1.5	38
77	Nitrosopumilus maritimus gen. nov., sp. nov., Nitrosopumilus cobalaminigenes sp. nov., Nitrosopumilus oxyclinae sp. nov., and Nitrosopumilus ureiphilus sp. nov., four marine ammonia-oxidizing archaea of the phylum Thaumarchaeota. International Journal of Systematic and Evolutionary Microbiology. 2017. 67. 5067-5079.	0.8	159
78	Primate TRIM5 proteins form hexagonal nets on HIV-1 capsids. ELife, 2016, 5, .	2.8	87
79	Phylogenomic analysis of <i>Candidatus</i> â€Izimaplasma' species: free-living representatives from a <i>Tenericutes</i> clade found in methane seeps. ISME Journal, 2016, 10, 2679-2692.	4.4	88
80	Author's reply. Nature Reviews Microbiology, 2016, 14, 600-600.	13.6	0
81	Chemotaxis cluster 1 proteins form cytoplasmic arrays inVibrio choleraeand are stabilized by a double signaling domain receptor DosM. Proceedings of the National Academy of Sciences of the United States of America, 2016, 113, 10412-10417.	3.3	55
82	Coarse-grained simulation reveals key features of HIV-1 capsid self-assembly. Nature Communications, 2016, 7, 11568.	5.8	134
83	Cryo-EM structure of a CD4-bound open HIV-1 envelope trimer reveals structural rearrangements of the gp120 V1V2 loop. Proceedings of the National Academy of Sciences of the United States of America, 2016, 113, E7151-E7158.	3.3	130
84	Coarse-Grained Molecular Dynamics Simulations of the Bacterial Cell Wall. Methods in Molecular Biology, 2016, 1440, 247-270.	0.4	3
85	Sporulation, bacterial cell envelopes and the origin of life. Nature Reviews Microbiology, 2016, 14, 535-542.	13.6	88
86	Architecture of the type IVa pilus machine. Science, 2016, 351, aad2001.	6.0	347
87	Dynamic Remodeling of the Magnetosome Membrane Is Triggered by the Initiation of Biomineralization. MBio, 2016, 7, e01898-15.	1.8	40
88	Diverse high-torque bacterial flagellar motors assemble wider stator rings using a conserved protein scaffold. Proceedings of the National Academy of Sciences of the United States of America, 2016, 113, E1917-26.	3.3	170
89	A new view into prokaryotic cell biology from electron cryotomography. Nature Reviews Microbiology, 2016, 14, 205-220.	13.6	86
90	Direct visualization of vaults within intact cells by electron cryo-tomography. Cellular and Molecular Life Sciences, 2015, 72, 3401-3409.	2.4	22

#	Article	IF	CITATIONS
91	Electron Cryotomography Studies of Maturing HIV-1 Particles Reveal the Assembly Pathway of the Viral Core. Journal of Virology, 2015, 89, 1267-1277.	1.5	56
92	Structural conservation of chemotaxis machinery across <scp>A</scp> rchaea and <scp>B</scp> acteria. Environmental Microbiology Reports, 2015, 7, 414-419.	1.0	100
93	The Caltech Tomography Database and Automatic Processing Pipeline. Journal of Structural Biology, 2015, 192, 279-286.	1.3	32
94	Coarse-grained simulations of bacterial cell wall growth reveal that local coordination alone can be sufficient to maintain rod shape. Proceedings of the National Academy of Sciences of the United States of America, 2015, 112, E3689-98.	3.3	50
95	Streptomyces: A Screening Tool for Bacterial Cell Division Inhibitors. Journal of Biomolecular Screening, 2015, 20, 275-284.	2.6	5
96	Escherichia coli Peptidoglycan Structure and Mechanics as Predicted by Atomic-Scale Simulations. PLoS Computational Biology, 2014, 10, e1003475.	1.5	92
97	Ultrastructure and complex polar architecture of the human pathogen Campylobacter jejuni. MicrobiologyOpen, 2014, 3, 702-710.	1.2	25
98	New Insights into Bacterial Chemoreceptor Array Structure and Assembly from Electron Cryotomography. Biochemistry, 2014, 53, 1575-1585.	1.2	91
99	Marine Tubeworm Metamorphosis Induced by Arrays of Bacterial Phage Tail–Like Structures. Science, 2014, 343, 529-533.	6.0	223
100	Correlated cryogenic photoactivated localization microscopy and cryo-electron tomography. Nature Methods, 2014, 11, 737-739.	9.0	201
101	Structure of bacterial cytoplasmic chemoreceptor arrays and implications for chemotactic signaling. ELife, 2014, 3, e02151.	2.8	112
102	Discovery of chlamydial peptidoglycan reveals bacteria with murein sacculi but without FtsZ. Nature Communications, 2013, 4, 2856.	5.8	123
103	The mobility of two kinase domains in the <i><scp>E</scp>scherichia coli</i> chemoreceptor array varies with signalling state. Molecular Microbiology, 2013, 89, 831-841.	1.2	59
104	Architecture of the major component of the type III secretion system export apparatus. Nature Structural and Molecular Biology, 2013, 20, 99-104.	3.6	200
105	The bacterial cytoskeleton: more than twisted filaments. Current Opinion in Cell Biology, 2013, 25, 125-133.	2.6	52
106	Architecture and assembly of the <scp>G</scp> ramâ€positive cell wall. Molecular Microbiology, 2013, 88, 664-672.	1.2	116
107	Polyphosphate Storage during Sporulation in the Gram-Negative Bacterium Acetonema longum. Journal of Bacteriology, 2013, 195, 3940-3946.	1.0	48
108	Electron cryotomography of ESCRT assemblies and dividing <i>Sulfolobus</i> cells suggests that spiraling filaments are involved in membrane scission. Molecular Biology of the Cell, 2013, 24, 2319-2327.	0.9	88

#	Article	IF	CITATIONS
109	Data management challenges in three-dimensional EM. Nature Structural and Molecular Biology, 2012, 19, 1203-1207.	3.6	49
110	A multidomain hub anchors the chromosome segregation and chemotactic machinery to the bacterial pole. Genes and Development, 2012, 26, 2348-2360.	2.7	154
111	The Helical MreB Cytoskeleton in Escherichia coli MC1000/pLE7 Is an Artifact of the N-Terminal Yellow Fluorescent Protein Tag. Journal of Bacteriology, 2012, 194, 6382-6386.	1.0	186
112	Bacterial chemoreceptor arrays are hexagonally packed trimers of receptor dimers networked by rings of kinase and coupling proteins. Proceedings of the National Academy of Sciences of the United States of America, 2012, 109, 3766-3771.	3.3	247
113	General Protein Diffusion Barriers Create Compartments within Bacterial Cells. Cell, 2012, 151, 1270-1282.	13.5	68
114	Electron tomography of cells. Quarterly Reviews of Biophysics, 2012, 45, 27-56.	2.4	138
115	Growth and Localization of Polyhydroxybutyrate Granules in Ralstonia eutropha. Journal of Bacteriology, 2012, 194, 1092-1099.	1.0	65
116	Peptidoglycan Remodeling and Conversion of an Inner Membrane into an Outer Membrane during Sporulation. Cell, 2011, 146, 799-812.	13.5	98
117	Long helical filaments are not seen encircling cells in electron cryotomograms of rod-shaped bacteria. Biochemical and Biophysical Research Communications, 2011, 407, 650-655.	1.0	75
118	Nanopods: A New Bacterial Structure and Mechanism for Deployment of Outer Membrane Vesicles. PLoS ONE, 2011, 6, e20725.	1.1	68
119	Activated chemoreceptor arrays remain intact and hexagonally packed. Molecular Microbiology, 2011, 82, 748-757.	1.2	38
120	Structural diversity of bacterial flagellar motors. EMBO Journal, 2011, 30, 2972-2981.	3.5	281
121	Alternative mechanism for bacteriophage adsorption to the motile bacterium <i>Caulobacter crescentus</i> . Proceedings of the National Academy of Sciences of the United States of America, 2011, 108, 9963-9968.	3.3	114
122	Microtubules in Bacteria: Ancient Tubulins Build a Five-Protofilament Homolog of the Eukaryotic Cytoskeleton. PLoS Biology, 2011, 9, e1001213.	2.6	108
123	Bactofilins, a ubiquitous class of cytoskeletal proteins mediating polar localization of a cell wall synthase in Caulobacter crescentus. EMBO Journal, 2010, 29, 327-339.	3.5	143
124	The metabolic enzyme CTP synthase forms cytoskeletal filaments. Nature Cell Biology, 2010, 12, 739-746.	4.6	262
125	Electron Cryotomography. Cold Spring Harbor Perspectives in Biology, 2010, 2, a003442-a003442.	2.3	69
126	Organization, Structure, and Assembly of α-Carboxysomes Determined by Electron Cryotomography of Intact Cells. Journal of Molecular Biology, 2010, 396, 105-117.	2.0	154

#	Article	IF	CITATIONS
127	Bacterial TEM. Methods in Cell Biology, 2010, 96, 21-45.	0.5	89
128	Correlated Light and Electron Cryo-Microscopy. Methods in Enzymology, 2010, 481, 317-341.	0.4	72
129	Plunge Freezing for Electron Cryomicroscopy. Methods in Enzymology, 2010, 481, 63-82.	0.4	108
130	Universal architecture of bacterial chemoreceptor arrays. Proceedings of the National Academy of Sciences of the United States of America, 2009, 106, 17181-17186.	3.3	320
131	Protein Filaments Caught in the Act. Science, 2009, 323, 472-473.	6.0	3
132	Fully automated, sequential tilt-series acquisition with Leginon. Journal of Structural Biology, 2009, 167, 11-18.	1.3	180
133	Nanogold as a Specific Marker for Electron Cryotomography. Microscopy and Microanalysis, 2009, 15, 183-188.	0.2	9
134	FcRn-mediated antibody transport across epithelial cells revealed by electron tomography. Nature, 2008, 455, 542-546.	13.7	150
135	Novel ultrastructures of <i>Treponema primitia</i> and their implications for motility. Molecular Microbiology, 2008, 67, 1184-1195.	1.2	44
136	Location and architecture of the <i>Caulobacter crescentus</i> chemoreceptor array. Molecular Microbiology, 2008, 69, 30-41.	1.2	111
137	A Self-Associating Protein Critical for Chromosome Attachment, Division, and Polar Organization in Caulobacter. Cell, 2008, 134, 956-968.	13.5	286
138	Fast nonlocal filtering applied to electron cryomicroscopy. , 2008, , .		157
139	Molecular organization of Gram-negative peptidoglycan. Proceedings of the National Academy of Sciences of the United States of America, 2008, 105, 18953-18957.	3.3	239
140	An Improved Cryogen for Plunge Freezing. Microscopy and Microanalysis, 2008, 14, 375-379.	0.2	273
141	The Structure of Isolated Synechococcus Strain WH8102 Carboxysomes as Revealed by Electron Cryotomography. Journal of Molecular Biology, 2007, 372, 764-773.	2.0	153
142	The structure of FtsZ filaments in vivo suggests a force-generating role in cell division. EMBO Journal, 2007, 26, 4694-4708.	3.5	340
143	How electron cryotomography is opening a new window onto prokaryotic ultrastructure. Current Opinion in Structural Biology, 2007, 17, 260-267.	2.6	86
144	Magnetosomes Are Cell Membrane Invaginations Organized by the Actin-Like Protein MamK. Science, 2006, 311, 242-245.	6.0	601

#	Article	IF	CITATIONS
145	Electron cryotomography sample preparation using the Vitrobot. Nature Protocols, 2006, 1, 2813-2819.	5.5	180
146	In situ structure of the complete Treponema primitia flagellar motor. Nature, 2006, 442, 1062-1064.	13.7	168
147	A "flip–flop―rotation stage for routine dual-axis electron cryotomography. Journal of Structural Biology, 2005, 151, 288-297.	1.3	61
148	Alignment Error Envelopes for Single Particle Analysis. Journal of Structural Biology, 2001, 133, 143-155.	1.3	40
149	Defocus-gradient corrected back-projection. Ultramicroscopy, 2000, 84, 57-64.	0.8	54
150	Single-particle selection and alignment with heavy atom cluster-antibody conjugates. Proceedings of the United States of America, 1998, 95, 9262-9267.	3.3	20
151	Structure of Wild Type Yeast RNA Polymerase II and Location of RPB4 and RPB7. Microscopy and Microanalysis, 1998, 4, 972-973.	0.2	1
152	Electron Cryotomography of Bacterial Secretion Systems. , 0, , 1-12.		0